We are IntechOpen, the world's leading publisher of Open Access books Built by scientists, for scientists

4,800
Open access books available

122,000
International authors and editors

135M
Downloads

Our authors are among the

154
Countries delivered to

TOP 1%
most cited scientists

12.2%
Contributors from top 500 universities

WEB OF SCIENCE™

Selection of our books indexed in the Book Citation Index in Web of Science™ Core Collection (BKCI)

Interested in publishing with us?
Contact book.department@intechopen.com

Numbers displayed above are based on latest data collected.
For more information visit www.intechopen.com

11

Fast-Response Organic Light-Emitting Diode for Interactive Optical Communication

Takeshi Fukuda[1] and Yoshio Taniguchi[2]
[1]*Department of Functional Materials Science, Saitama University*
[2]*Shinshu University*
Japan

1. Introduction

In recent years, many types of electronic equipment have come into wide use in our lives. Especially, mobile phones and personal computers have been widely used by many people, and this fact causes the drastically change of our lives. In addition, we can connect global networks using mobile phones and personal computers, and we can get much information in a short time without moving. Nowadays, several mobile networks are widely used, such as, Bluetooth, ultra wideband, ZigBEE, and so on. Furthermore, the global computer networks will be used unconsciously without thinking the connection in near future, and many researchers demonstrated unique concepts of intuitive interface modules. (Morrison et al., 2005; Wilson et al., 2007; Mignonneau et al., 2005) To realize an intuitive interface module between real the world and the global computer network, we proposed the free space visible optical communication system utilizing organic light-emitting diodes (OLEDs) as a transceiver module and organic photo-diodes (OPDs) as a receiver module, as shown in Fig. 1. In this system, we can get information from the OLED by touching the emitting area, and the emitting area of the OLED is large enough to connect without the precious alignment between the OLED and the OPD.

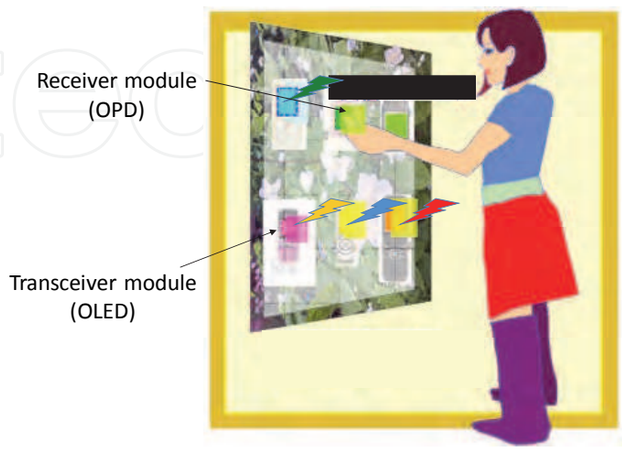

Fig. 1. Concept of the interactive visible optical communication system using the OLED and the OPD with the high response speed.

By now, several research groups demonstrated OLEDs and OPDs with the high response speed for the novel application of the optical communication, and the response speed of more than Mbps has been achieved by optimizing the device structure. (Shimada et al., 2006; Morimune et al., 2006) The reported optical communication system consists of an optical fiber to transmit optical signals generated from the OLED to the OPD. In generally, a core diameter of the multimode optical fiber is several 100 μm. (Koike, 2008) Even though the optical signal reaches far from the OLED, the high accuracy alignment between the OLED/OPD and the optical fiber is necessary to achieve the efficient optical communication. Furthermore, the emitting area of the OLED and the receiving area of the OPD can be controlled by changing the deposition areas of electrodes, which sandwiches organic layers. Therefore, we have proposed that the free space optical data transmission is suitable for the next generation visible optical communication system due to the alignment-less connection. The visible light of the OLED announces the connection point, and everyone can get optical information by touching the visible light using the receiver module (OPD). Moreover, OLEDs and OPDs can be fabricated by printing processes, resulting in the low-fabrication cost and the flexible devices. (Mori et al., 2003; Ooe et al., 2003)

OLEDs have attracted a great deal of public attention as visible light sources of flat panel displays and lightings. In recent years, several breakthroughs have led to significant enhancements of performances in OLEDs, such as the improvement in the charge-carrier balance, (Tsutsui, 1997) the low-work function electrode material, (Parker, 1994) the efficient injection of the electron from a metal cathode to an adjacent organic layer by inserting an electron injection layer (EIL), (Kido et al., 1998; Hung et al., 1997; Stöβel et al., 2000; Kin et al., 2006) the high carrier mobility of electron/hole transport materials, (Ichikawa et al., 2006; Uchida et al, 2001) the high efficiency fluorescence and phosphorescence emitting materials. (Tang et al., 1987; Adachi et al., 2001; Cao et al., 1999; Xu et al., 2003) In the case of the visible optical communication system, the response speed is an important factor for the practical application. The reported cutoff frequency of the output power, which indicates the response speed, has been achieved up to 25 MHz for the OLED with a small area of 300 μm circle. (Kim et al., 2006) However, the large emitting area of the OLED is necessary for our proposed institutive visible optical communication system.

We investigated the response speed of the OLED by changing device parameters, such as the device area (capacitance of the organic layer), the fluorescence lifetime of the organic emitting material, (Fukuda et al., 2007) the thickness of hole/electron transport layers (HTL and ETL) corresponding to the carrier transport time from the electrode to the EML, the energy gap at a metal/organic interface (Fukuda et al., 2007), the combination of the host-guest materials used as the emitting layer (EML) (Fukuda et al., 2009), and the effect of the hole blocking layer (Fukuda et al., 2007). In this chapter, we show the experimental result of the fast response OLED. Then, we investigated the organic-inorganic hybrid device using ZnS as the ETL (Fukuda et al., 2008a). This is because that the response speed of the OLED is limited by the low electron mobility of the organic ETL material, and ZnS has higher electron mobility than organic materials. Finally, we demonstrated the intuitive optical communication system utilizing the OLED as a transceiver. In this system, we succeeded in the transmission of the pseudo-random signal with 1 Mbps and the movie files with 230 kbps, when the pen-type photo-diode is touched the emitting area of the OLED.

2. Limiting factor of the response speed of the OLED

The conventional OLED consists of a transparent anode, several organic layers, and a metal cathode, as shown in Fig. 2. The each organic layers are called as the hole injection layer (HIL), the HTL, the EML, the HBL, and the HTL. The names of these organic layers indicate their functions of the operation mechanism. When the voltage is applied between the transparent anode and the metal cathode, holes and electrons (carriers) are injected into the organic layers, respectively. Then, these injected holes and electrons transport into the HTL and the ETL, respectively. Finally, the carriers recombine into the EML, resulting in the generation of light. The generated light comes out from a transparent anode and a transparent substrate. That is to say the response speed of OLEDs is limited by the time from the applying voltage to the generation of light caused by the carrier recombination. We examined the details of these processes and the method to improve the response speed of the OLED.

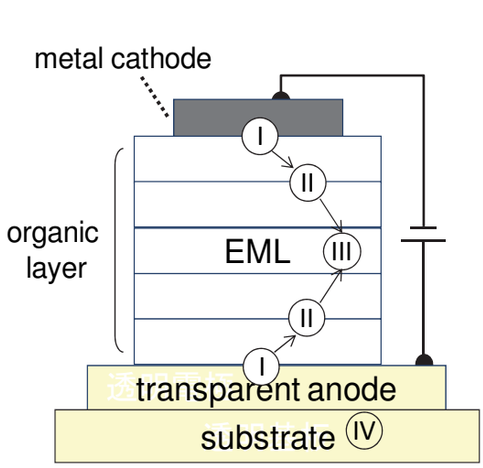

Mechanism and limiting factor

I. Holes and electrons are infected from the transparent anode ant the metal cathode, respectively.
⇒Energy barrier at metal/organic interface

II. Holes and electrons transport to the EML
⇒Carrier mobility of organic material

III. Carrier recombination in the EML
⇒Fluorescence lifetime of EML

IV. Light is taken out from the substrate

Fig. 2. Cross sectional view of the conventional OLED structure and limiting factors of the transmission speed of the OLED.

3. Fabrication process of the OLED and the experimental setup to estimate the response speed of the OLED

The fabrication process of the OLED is described in the following sentence. OLEDs were fabricated on glass substrates covered with a patterned indium tin oxide (ITO) anode. The thickness of the ITO layer was 150 nm. The prepared glass substrates were cleaned in deionized water, detergent, and isopropyl alcohol sequentially under ultrasonic waves, and then treated with oxygen plasma for 5 min. Next, several organic layers, an EIL and a metal cathode were thermally deposited successively using a conventional vacuum deposition system at a base pressure of below 5.0×10^{-6} Torr. Deposition rates were maintained at 0.8-1.0 Å/s for both the HTL and the ETL, 5.0 Å/s for both the EML and the metal cathode, and 0.1-0.2 Å/s for the EIL as determined using a quartz crystal monitor.

To evaluate the response speed of the OLED, we measured the relative EL intensity as a function of the frequency of an applied sine wave voltage. Figure 3 shows the schematic configuration of the experimental setup. The sine wave and bias voltages were applied to the OLED using a programmable FM/AM standard signal generator (KENWOOD, SG-7200)

and a DC power supply (ISO-TECH, IPS-3610D), respectively. The amplitude of the sine wave voltage was controlled using an attenuator (Furuno Electric, VHF-STEP) and a high speed amplifier (ARF Japan, ARF-15237-25). In addition, several resistances and capacitances were used to reduce the frequency dependence of the amplitude of the applied sine wave voltage, as shown in Fig. 3.

The generated light wad guided into a plastic optical fiber (Moritex, PJR-FB250) with the diameter of 250 μm. Then, the output EL intensity was observed using an avalanche photodiode (Hamamatsu Photonics, S5343) and an oscilloscope (Yokogawa Electronic, DL-1740). The frequency dependence of EL intensity was measured by changing the modulation frequency of the sine wave voltage from 100 kHz to 10 MHz. In addition, the rise and decay times of output EL intensity were also measured while applying a pulse voltage with a width of 1 μs to investigate the transient properties of the OLED. The rise and decay times were defined as the times required for the optical response to change from 10% to 90% and from 90% to 10% of the maximum EL intensity, respectively. We also measured the luminance-current density-voltage characteristics of the OLED using a source measure unit (Hewlett-Packard, HP4140B) and a luminance color meter (Topcon, BM-7).

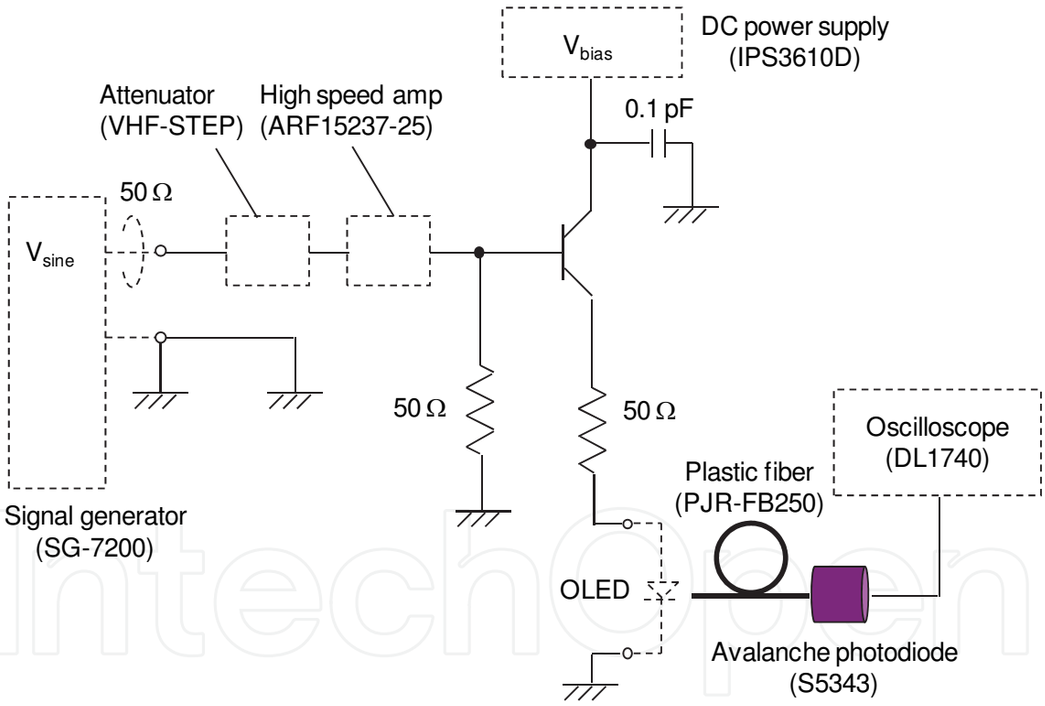

Fig. 3. Cross sectional view of the conventional OLED structure and limiting factors of the transmission speed of the OLED.

4. Response speed of the OLED

4.1 Device area (capacitance of the organic layer)

The conventional OLED consists of several organic layers with a total thickness of less than 200 nm due to the low carrier mobility of organic materials, resulting in the large capacitance of an emitting area. The capacitance of an emitting area is well known to affect pulse voltage-

transient current characteristics, and the large capacitance of the organic layer causes the long decay time of the transient current while applying a pulse voltage. (Wei et al., 2004) Therefore, the lower capacitance, corresponding to the smaller emitting area, is required for the high response speed of OLEDs. By now, previous papers demonstrated that the response speed of the OLED increases by reducing the capacitance of the emitting area. (Kajii et al., 2002a)
To investigate the influence of the emitting area on the response speed of the OLED, we used 4,4'-bis[*N*-(1-napthyl)-*N*-phenyl-amino]-biphenyl (α-NPD) as the HTL, 6,11,12-tetraphenyltetracene (rubrene) as the dopant in the EML, and tris(8-hydroxyquinoline) aluminium (Alq_3) as the EML and the ETL. Figure 4 shows molecular structures of used organic materials. The device structure is ITO 150 nm/α-NPD 40 nm/rubrene:Alq_3(0.5wt%) 20 nm/Alq_3 40 nm/LiF 0.4nm/MgAg (9:1) 150 nm/Ag 20nm for the device A and ITO 150 nm/α-NPD 40 nm/Alq_3 60 nm/LiF 0.4nm/MgAg (9:1) 150 nm/Ag 20nm for the device B. In addition, the emitting area was changed from 0.2 to 1.5 mm² to investigate the influence of the emitting area on the response speed of the OLED.

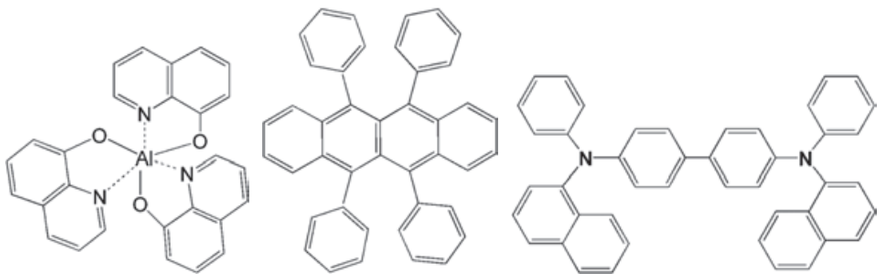

Alq_3 rubrene a-NPD

Fig. 4. Molecular structures of organic materials (α-NPD, rubrene and Alq_3)

Figure 5 shows the relative output EL intensity as a function of modulation frequency for the two OLEDs, that is, devices A and B with rubrene doped Alq_3 and Alq_3 as EMLs, respectively. The sine wave voltage was 7 V and the bias voltage was 5 V. Here, the EL intensities at various modulation frequencies are normalized with respect to the EL intensity at a frequency of 100 kHz. It was observed that the relative EL intensity of device A with the rubrene doped Alq_3 EML is higher than that of device B, which has the Alq_3 EML. This result indicates that the device A has a higher response speed than the device B. This result can be explained by the fluorescence lifetime of the EML. (Kajii et al., 2002b) The fluorescence lifetime of rubrene doped Alq_3 (0.5wt%) and non-dope Alq_3 were 10 ns and 16 ns, respectively. (Fukuda et al., 2007b) Therefore, the response speed of the OLED was improved by doping rubrene in the EML.
The cutoff frequency of the device A with the emitting area of 1.2 mm² was 4.0 MHz, and the 2-times faster cutoff frequency (8 MHz) was achieved when the emitting area was 0.2 mm. The cutoff frequency corresponds to the responses speed of the OLED; therefore, this result indicates that the response speed of the OLED was improved with decreasing capacitance of the emitting area. In the case of the institutive optical communication system, the large emitting area is important factor to connect between the OLED and the OPD. Therefore, the response speed of the OLED is necessary to improve by optimizing other device parameters.

4.2 Thickness of hole/electron transport layers (carrier injection time)

In generally, the carrier mobility of organic materials is much lower than that of inorganic materials. This fact causes the long decay time from the carrier injection to the generation of

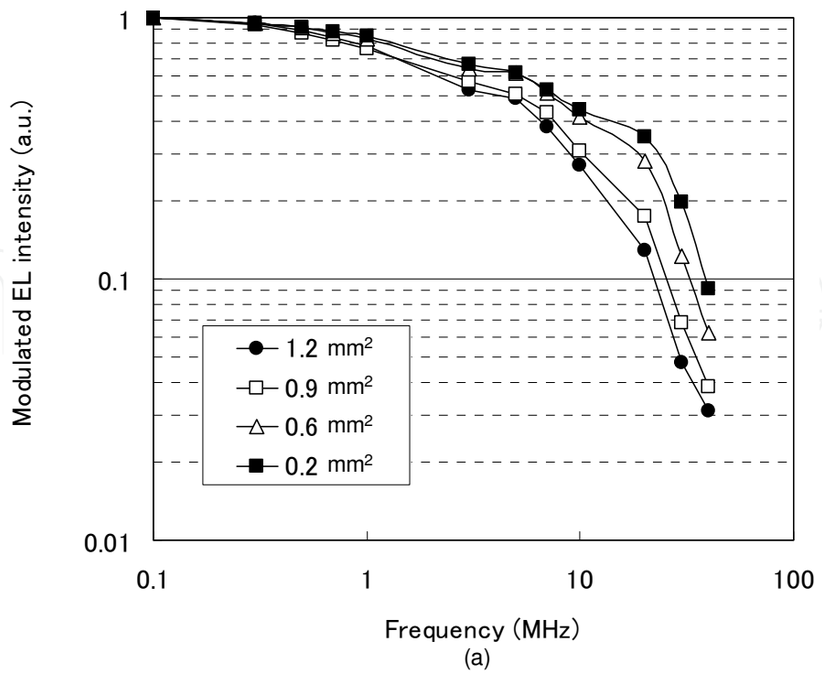

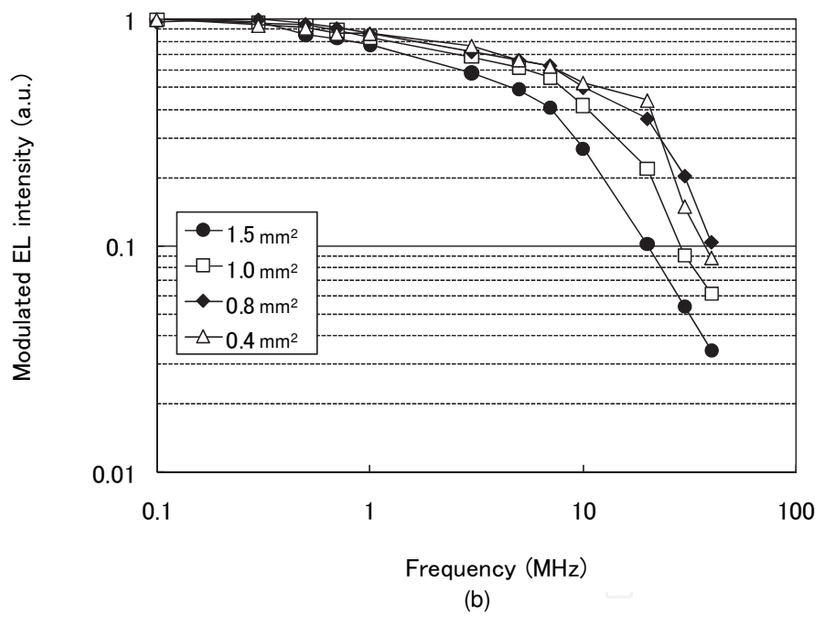

Fig. 5. Relative EL intensity while applying the sine wave voltage for (a) the device A with rubrene:Alq_3 and (b) the device B with Alq_3 as EMLs.

light, resulting in the slow response time of the OLED. In addition, the carrier transport time from the electrode to the EML is related with the thickness of HTL and the ETL. Here, we show the relationship between the thicknesses of the HTL/ETL and the response speed of the OLED. (Fukuda et al., 2007e)

The device structure is ITO 150 nm/α-NPD 40 nm/rubrene:Alq_3(0.5wt%) 20 nm/Alq_3 10-40nm/LiF 0.4nm/MgAg (9:1) 150 nm/Ag 20nm. Active areas were decided as the

sandwiched region of ITO/MgAg, and those of all the devices were fixed at 1 mm^2. The detail of the measurement is described in the above-mentioned section.

Figure 6(a) shows the relationship between the applied pulse voltage and the rise time of output EL intensity of OLEDs with different thicknesses in the ETL. The thicknesses of the ETLs were 10 nm, 20 nm, 30 nm, and 40 nm. As clearly shown in Fig. 6(a), the rise time decreased with decreasing thickness of the ETL. The electron injection time is calculated from the electron mobility, the thickness, and the applied electric field. The electron mobility of Alq_3 is about 10^{-5} cm^2/Vs (Barth et al., 2001). Therefore, we can estimate the electron injection time of 450 ns, 250 ns, 150 ns, and 50 ns for OLEDs with thicknesses in 40 nm, 30 nm, 20 nm, and 10 nm, respectively. The measurement results of the rise times were longer than the estimated electron injection times. These differences are considered to be caused by the energy gap at metal/organic interface and the capacitance of the organic layer. In addition, the decay time was also reduced with decreasing thickness of the ETL. In addition, the decay time shown in Fig. 6(b) also decreased with decreasing thickness of the ETL. This result indicates that the carrier injection time mainly affect the decay time of the output EL intensity while applying the high speed pulse voltage.

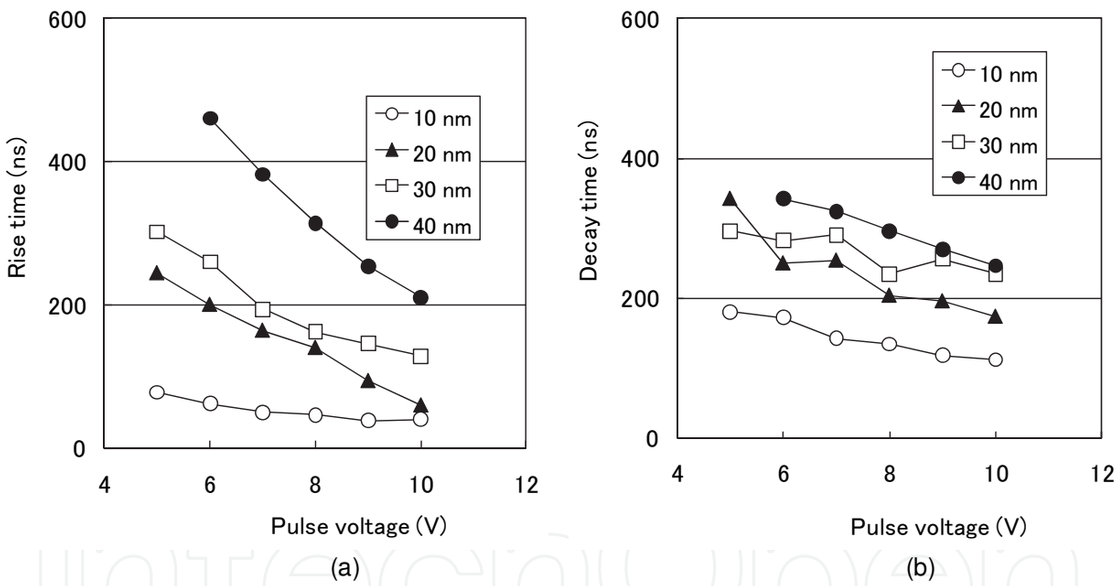

Fig. 6. Influence of the pulse voltage on (a) rise and (b) decay times of the OLEDs with different thickness of the ETL (Alq_3). (Fukuda et al., 2007e)

Figure 7 shows the relative EL intensity of OLEDs with different thicknesses of the ETLs when the sine wave voltage was applied to the device. The sine wave voltage was 8 V and the bias voltage was 5 V. The relative EL intensity at the high frequency region increased with decreasing the thickness of the ETL. This result indicates that the response speed increased with decreasing thickness of the ETL, which corresponds to the electron travelling length from the metal cathode to the EML.

On the other hand, the rise time was little influenced by the thickness of the HTL ranged from 20 nm to 40 nm, as shown in Figs. 8(a). The device structure was ITO 150 nm/α-NPD 20-40 nm/rubrene:Alq_3(0.5wt%) 20 nm/Alq_3 10nm/LiF 0.4nm/MgAg (9:1) 150 nm/Ag

20nm. Active areas were decided as the sandwiched region of ITO/MgAg, and those of all the devices were fixed at 1 mm^2.

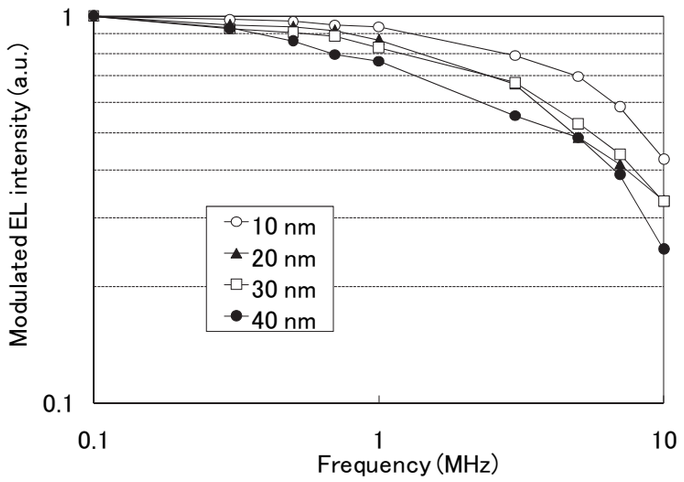

Fig. 7. Relative EL intensity while applying the sine wave voltage for OLEDs with different thicknesses of the ETLs. (Fukuda et al., 2007e)

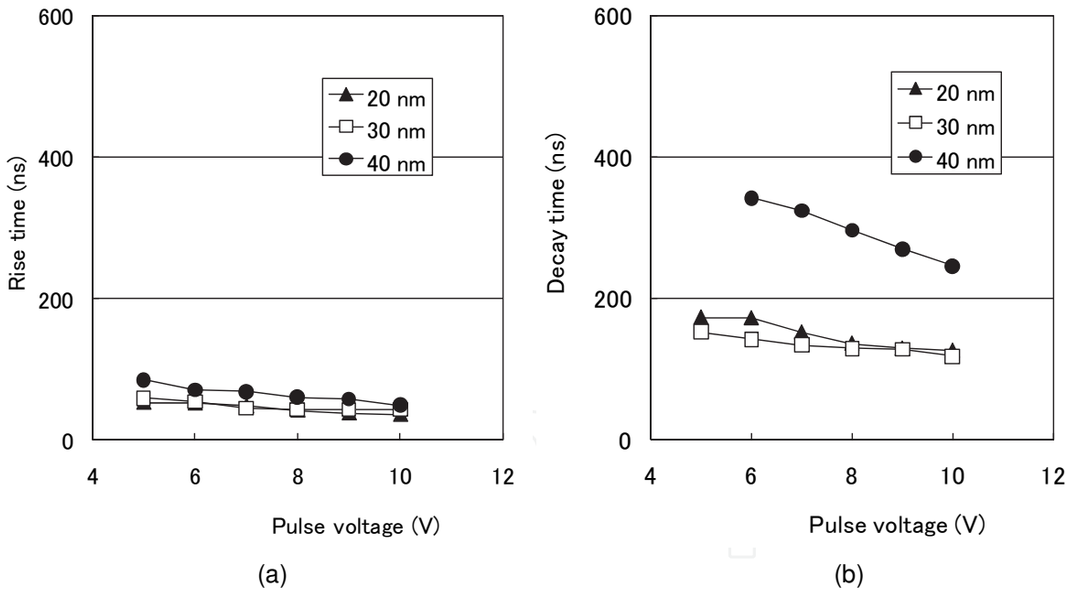

Fig. 8. Influence of the pulse voltage on (a) rise and (b) decay times of the OLEDs with different thickness of the HTL (α-NPD). (Fukuda et al., 2007e)

The thickness of the ETL (Alq_3) was 10 nm, and the response speed of the OLED was almost same for all the devices. This is because that the electron mobility of Alq_3 is much lower than the hole mobility of α-NPD. These experimental results indicate that the thickness of the ETL mainly limits the response speed of OLEDs owing to the low electron mobility of Alq_3 used as the ETL (Fukuda et al., 2007e).

4.3 Energy gap between metal the cathode and the adjacent organic layer

In generally, holes and electrons (carriers) are injected from an anode and a cathode, respectively. The injection efficiency of carriers is defined by the energy level difference between an electrode and an adjacent organic layer (Kampen et al., 2004). Therefore, the low energy gap at the electrode/organic interface is necessary to realize efficient carrier injection and to reduce the drive voltage of OLEDs. By now, many researchers have investigated, such as the surface treatment of the indium tin oxide (ITO) layer used as a transparent anode (Nüesch et al., 1998; Hatton et al., 2001), the low work function metal cathode, (Parker, 1994) and hole/electron injection layers at the electrode/organic interface. (Kido et al., 1998; Hung et al., 1997; Stöβel et al., 2000; Kin et al., 2006) Especially, the metal/organic interface has a large energy gap, and Schottky barrier is formed at the metal/organic interface. As a result, the efficiency of injecting electrons into an organic layer form a metal cathode is low, and the high drive voltage is necessary. Furthermore, the large energy gap at metal/organic interface causes the decrease in the response speed of the OLED (Ichikawa et al., 2003; Fukuda et al., 2007d). In addition, the carrier injection efficiency at the organic/organic interface is also important factor for high speed OLEDs. (Fukuda et al., 2007c)

The thicknesses of the organic layers are 40 nm for α-NPD, 20 nm for rubrene-doped Alq_3, and 30 nm for Alq_3. In addition, we employed three species of metal cathodes of 100 nm thickness, namely, Ca/Al, Al, and MgAg (9:1 w/w)/Ag for devices C, D and E, respectively. To investigate the effects of an inserted EIL, we fabricated a similar set of OLEDs using a thin 8-hydroxyquinolinato lithium (Liq) layer with thickness of 0.4 nm as an EIL. We also used Ca/Al, Al and MgAg (9:1 mass ratio)/Ag as metal cathodes for devices F, G, and H, in which Liq was inserted between the metal cathode and the ETL. The current efficiency of the OLEDs with Liq is less sensitive to a change in EIL (Liq) thickness than that of OLEDs with the conventional EIL material of LiF, resulting in their suitability for mass production. (Zheng et al., 2005). The active areas of all the OLEDs were fixed at 1 mm^2.

Figure 9(a) shows the relationship between the relative EL intensity and the frequency of the applied sine wave voltage for the three OLEDs (devices C, D, and E). The sine wave voltage was 7 V and the bias voltage was 5 V. Here, the EL intensities at various frequencies are normalized with respect to the EL intensity at a frequency of 100 kHz. It was observed that the relative EL intensity of device C with the Ca/Al cathode was higher than those of devices D and E, which have Al and MgAg/Ag cathodes, respectively. The relative EL intensity at the high frequency region corresponds to the response speed of the OLED. Therefore, this result indicates that device C has a higher response speed than devices D and E. The cutoff frequency of device C was 8.5 MHz, while those of devices D and E were 1.3 and 4.2 MHz, respectively.

Figure 9(b) shows the influence of the barrier height at the metal/organic interface on the cutoff frequency. Here, the barrier height was calculated to be the difference between the work function of the metal cathode and the LUMO level of Alq_3 used as the ETL. The LUMO level of Alq_3 was 3.1 eV and work functions of metal cathodes were 3.0, 4.3, and 3.6 eV for Ca, Al, and MgAg, respectively. Therefore, the barrier heights were estimated to be 0.1, 1.2, and 0.5 eV for devices C, D, and E, respectively. The cutoff frequency increased with decreasing barrier height, which affects the efficiency of injecting electrons into the organic layer from the metal cathode. The cutoff frequency relates the response speed of the OLED; therefore, the response speed increases with decreasing barrier height at the metal/organic interface.

Figure 10 shows the relationship between the frequency of sine wave voltage and the relative EL intensity for the three EIL (Liq)-inserted OLEDs, that is, devices F, G, and H with

Ca/Al, Al, and MgAg/Ag as metal cathodes, respectively. The response speed of the OLED also increased when the low-work function metal electrode was used for the EIL-inserted OLED. The cutoff frequency of device F was observed to be about 11.2 MHz, while those of devices G and H were approximately 6.7 and 8.8 MHz, respectively. By comparing Fig. 9(a), we found that the cutoff frequency increased by inserting Liq layer for all the devices with the different cathode materials. Here, Li has low work function of 2.9 eV, and thus appears to be a good candidate for injecting electrons into the Alq_3 layer. It is known that diluted Li-metal alloys can act a cathode and exhibit much better transient characteristics than a pure metal cathode. (Zheng et al., 2005).

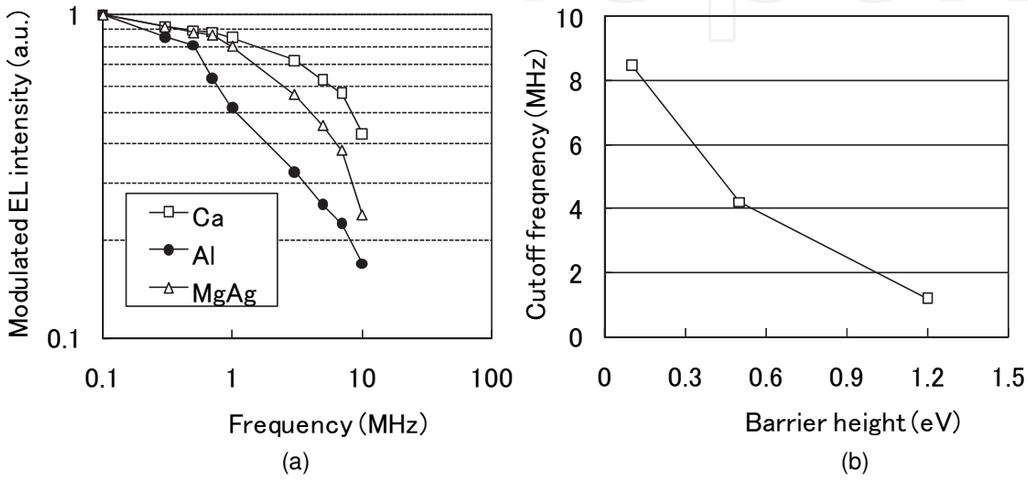

Fig. 9. (a) Frequency dependence of relative EL intensity for devices C, D, and E with Ca, Al, amd MgAg as metal cathodes, respectively. (b) Relationship between cutoff frequency and barrier height at metal cathode/Alq_3 interface. The cutoff frequency was calculated from the experimental result in Fig .9(a). (Fukuda et al., 2007c)

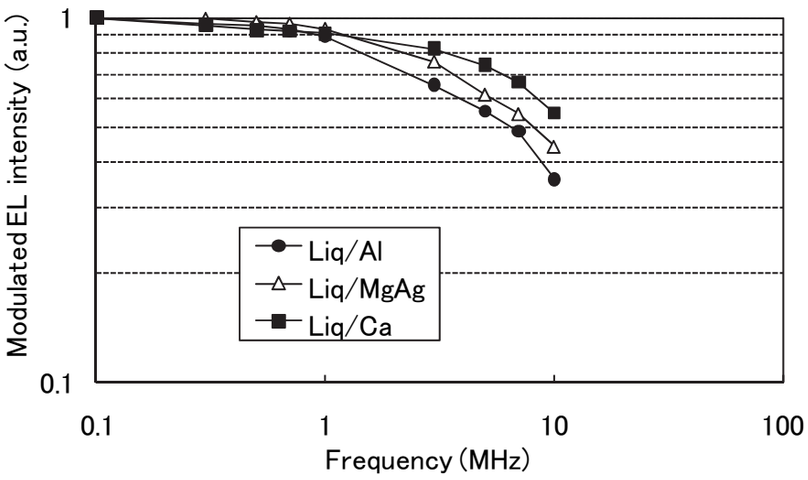

Fig. 10. Frequency dependence of relative EL intensity for devices F, G, and H with Ca, Al, and MgAg as metal cathodes, respectively. (Fukuda et al., 2007c)

4.4 Influence of fluorescence lifetime of EML and response speed of OLED

The fluorescence life time of organic emitting materials is important factor to determine the response speed of the OLED. (Kajii et al., 2002b) Therefore, we investigated the direct influence of the fluorescence lifetime on the response speed of the OLED. (Fukuda et al., 2007b)

We fabricated organic neat films on glass substrates by a conventional thermal evaporation system at a base pressure of below 5.0×10^{-6} Torr. The glass substrates were cleaned in deionized water, detergent, and isopropyl alcohol sequentially under ultrasonic waves, and then treated with 50 W oxygen plasma for 5 minutes just before use. Finally, the following 10 species of organic materials were deposited on glass substrates, and molecular structures of these organic materials are shown in Fig. 11. The used organic materials were 1,4-bis[2-[4-[*N*,*N*-di(*p*-tolyl)amino]phenyl]vinyl]benzene (DSB), 2-(4-tert-butylphenyl)-5-(4-biphenylyl)-1,3,4-oxadiazole (PBD), (3-(2-benzothiazolyl)-*N*,*N*-diethylumbelliferylamine (coumarin 6), 4,4'-(bis(9-ethyl-3-carbazovinylene)-1,1'-biphenyl (BCzVBi), 4,4-bis(2,2-ditolylvinyl)biphenyl (DPVBi), α-NPD, 4,4'-bis[9-dicarbazolyl]-2,2'-biphenyl (CBP), Alq_3, doped Alq_3, rubrene doped Alq_3, Pyrromethen 567 doped Alq_3, 4-(dicyanomethylene)2-methyl-6-(julolidin-4-yl-vinyl)-4H-pyran (DCM2), 4,7-diphenyl-1,10-phenanthroline (BPhen), Bis-(2-methyl-8-quinolinolate)-4-(phenylphenolato)aluminum (BAlq), Perylene, and rubrene.

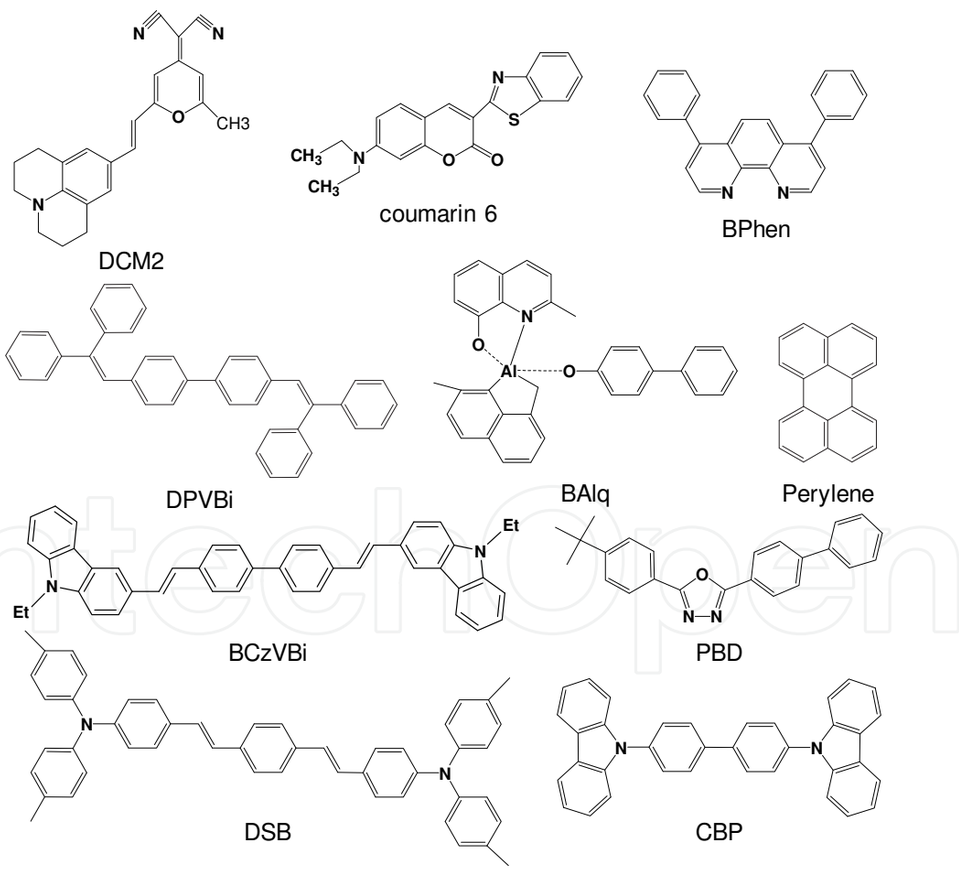

Fig. 11. Molecular structures of used organic materials.

After deposition of organic neat films, we measured fluorescence lifetimes of all the organic films by a femtosecond pulse laser (THALES Laser, Bright). After passing through the

second harmonic generator, the center wavelength and the pulse width of the femtosecond pulse laser were 390 nm and 112 femtosecond, respectively. All the organic films radiated photoluminescences (PLs), when the femtosecond pulse laser was irradiated. The radiated PL was captured with a spectrometer and a streak camera (Hamamatsu Photonics, A5760), then time-resolved PL spectra were measured. Finally, Mono-exponential fitting was employed to derive the FL from the measured time-resolved PL intensity.

The frequency dependence of PL intensity was measured to investigate the direct relationship between the cutoff frequency of PL intensity and the fluorescence lifetime of the organic neat film. A schematic configuration of an experimental setup is shown in Fig. 12. The organic neat film was excited by the violet laser diode (NDHV220APAE1-E, Nichia corp.). The center wavelength of the excited violet laser diode was 405 nm, and the all the organic neat film absorbs the excited light. In addition, the violet laser diode was operated by a high-frequency sine wave voltage utilizing the programmable FM/AM standard signal generator (SG-7200, KENWOOD). And then, PL intensity was observed using the avalanche photo diode (S5343, Hamamatsu Photonics), which was located perpendicular to the optical axis of the laser diode, as shown in Fig. 12.

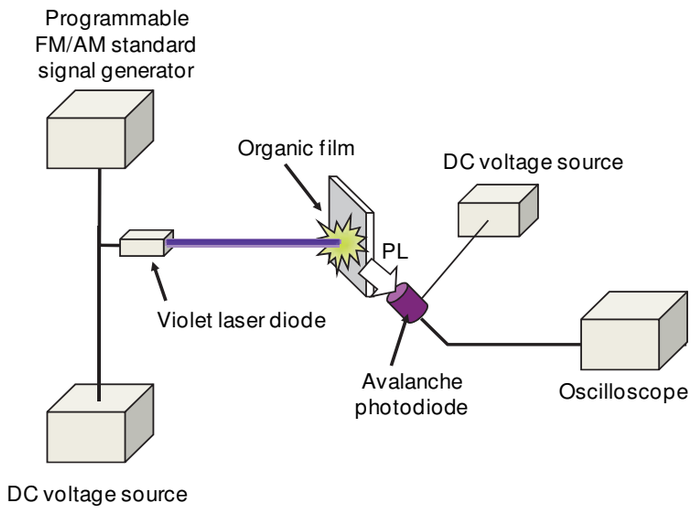

Fig. 12. Schematic configuration of the experimental setup to estimate the influence of the relative PL intensity while irradiating the violet laser diode.

As a result, the frequency dependence of PL intensity was estimated by changing the modulation frequency of the violet laser diode. Moreover, PL spectra were measured by the spectrophotometer (USB 2000, OceanOptics Company) also located perpendicular to the optical axis of the laser diode.

Figure 13(a) shows the influence of PL intensity on the frequency of the violet laser diode for two organic materials, DSB and Alq_3. For both organic films, PL intensity decreases with increasing frequency of the violet laser diode due to the decay time of the PL. This experimental result showed that cutoff frequencies were 160 MHz and 20 MHz for DSB and Alq_3, respectively. The difference of the cutoff frequency can be explained by the fluorescence lifetime of the organic material. The fluorescence lifetimes of DSB and Alq_3 were 0.2 ns and 16.0 ns, respectively. Therefore, the long fluorescence lifetime Alq_3 of causes the decreased cutoff frequency.

Figure 13(b) shows the relationship between the cutoff frequency of PL intensity and the fluorescence lifetime of the organic emitting material. This result is a consequence of fluorescence lifetimes without the influences of the capacitance and the carrier mobility, which are known to affect the response speed of the OLED. Therefore, we can estimate the direct influence of the fluorescence lifetime on the response time of the OLED. The transient characteristic of PL is strongly dependent on the fluorescence lifetime, and the response is considered to increase utilizing the short fluorescence lifetime of the organic material as a light-emitting layer of OLEDs. The highest cutoff frequency of PL intensity can reach about 160 MHz using one substituted phenyl/vinyl compound, DSB, of which the fluorescence lifetime was 0.2 ns.

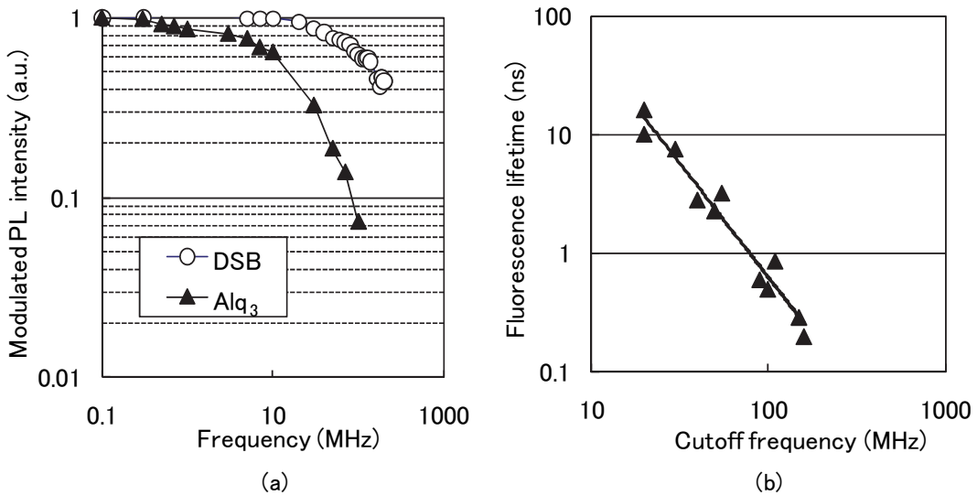

Fig. 13. (a) Relationship between the frequency of the irradiated violet laser diode and the relative PL intensity for DSB and Alq_3 neat films. (b) Influence of the cutoff frequency of the experimental result in Fig. 13(a) on the fluorescence lifetimes of organic neat films. (Fukuda et al., 2007b)

4.5 Combination of host-guest materials in EML

In the previous chapter, the fluorescence lifetime of the EML is important factor to realize the fast response speed of the OLED. In addition, the efficient energy transfer from the host material to the guest material is also key parameter for the increased response speed. (Fukuda et al., 2009)

To investigate the response speed of OLEDs with different combinations of host-guest materials, we fabricated three devices, referred as devices I, J, and K. The guest materials of devices I, J, and K were DSB, DPVBi, and BCzVBi, respectively. The device structure was α-NPD 40 nm/EML 20 nm/bathocuproine (BCP) 10 nm/Alq_3 20 nm/LiF 0.4 nm/MgAg (9:1 w/w) 100 nm/Ag 50 nm. Three organic emitting materials were choosed as DSB (device I), DPVBi (device J), and BCzVBi (device K) doped with CBP at 0.5 wt.%, respectively Emitting areas of all the devices were fixed at 1 mm^2.

Figures 14(a) and (b) show rise and decay times of the output EL intensity while applying the pulse voltage with the duration of 1 μs. The bias voltage was fixed at 6 V and the pulse voltage was ranged from 5 to 10 V. Both rise and decay times decreased with increasing

pulse voltage due to the high carrier mobility at the high electric field. In addition, the rise times of devices I (DSB), J (DPVBi), and K (BCzVBi) were 58, 345, and 257 ns at the pulse voltage of 5 V, respectively. The measured rise times were larger than the decay time of all the devices. In generally, the large capacitance of organic layers limits the response speed of OLEDs owing to the large emitting area and the thinness of organic layers compared to semiconductor emitting devices. (Kajii et al., 2002a) However, the rise time is same as the decay time when only the capacitance affects the response speed of the OLED. Therefore, we can conclude that the rise time of optical response is primarily associated with the carrier dynamics between the applying voltage and the generation of light. Furthermore, the fluorescence lifetime of DSB:CBP, DPVBi:CBP, and BCzVBi:CBP neat films at the concentration of 0.5 wt.% were 1.4, 1.6, and 0.8 ns, respectively. These values were estimated time-resolved PL intensity using a femtosecond pulse laser with the center wavelength of 390 nm and a streak camera. Such short fluorescence lifetimes were assumed to give little effect on response speed of device. (Fukuda et al., 2007b)

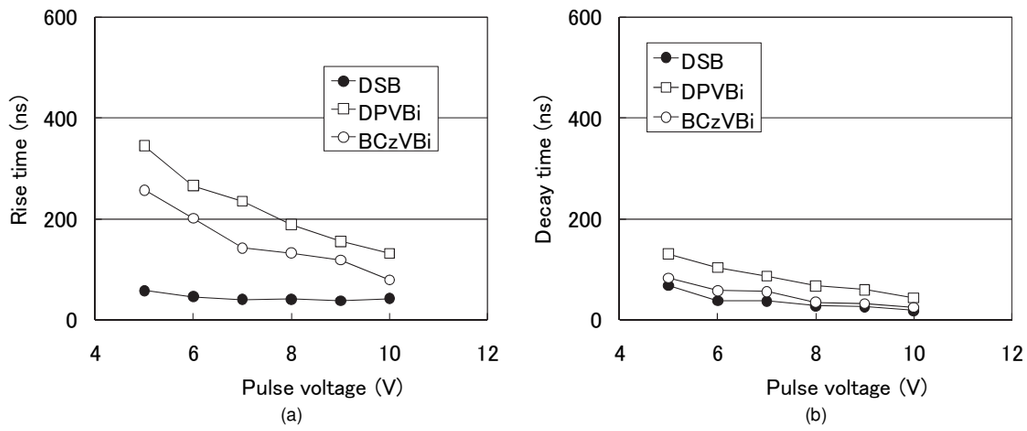

Fig. 14. (a) Rise and (b) decay times of the output EL intensity while applying the pulse voltage for three kinds of devices with different guest materials. (Fukuda et al., 2009)

Figure 15 shows absorption spectra of organic neat thin films of guest materials (DSB, DPVBi, and BCzVBi) and the PL spectrum of the CBP neat film. The PL spectrum of CBP showed the peak wavelength at 411 nm, and the PL intensity rapidly decreased in both shorter and longer wavelengths. The guest materials had peculiar absorption bands at the violet wavelength region. The peak wavelengths of absorption spectra of DSB, DPVBi, and BCzVBi were 418, 354, and 372 nm, respectively. Based on previous researches, the energy transfer efficiency of dye-doped OLEDs depends on the overlap integral of the emission spectrum of the host material and the absorption spectrum of the guest material. (Dexter, 1953; Eisenthal et al., 1953). The measured spectral overlap was different from each combination of the host-guest system, and the largest spectral overlap was achieved using DSB as a guest material. Therefore, efficient Förster energy transfer from the host material to the guest material is considered to be realized in the case of DSB doped CBP. As a result, the response speed of the OLED was also improved using DSB.

4.6 Organic-inorganic hybrid device

In the previous section, we showed that the low electron mobility of the ETL prevents the improved response speed of the OLED. (Fukuda et al., 2007e) In this section, we

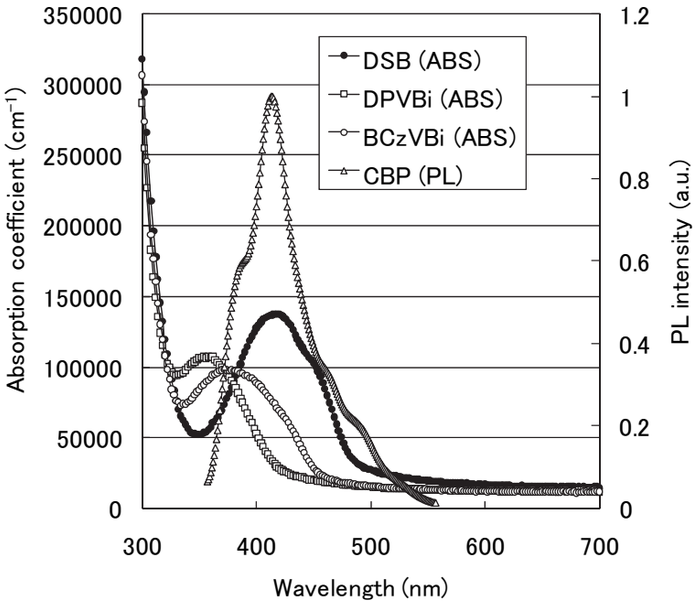

Fig. 15. Absorption spectra of DSB, DPVBi, and BCzVBi neat films and the PL spectrum of the CBP neat film. (Fukuda et al., 2009)

demonstrated organic-inorganic hybrid light-emitting diode, of which ZnS was used as the ETL. The ZnS layer has higher electron mobility compared to the organic electron transport material. Therefore, higher response speed can be realized compared to the OLED even though the emitting area is large. (Fukuda et al., 2008a) This fact indicates that such a device can be applicable for the institutive visible optical communication system.

Each layer consisted of α-NPD as an HTL, CBP doped with 0.5 wt% BCzVBi as an EML, and ZnS (device L) and Alq_3 (device M) as ETLs. Here, the fluorescence lifetime of BCzVBi was 0.6 ns, and it was short enough to realize the fast response speed. The thicknesses were 40 nm for α-NPD, 20 nm for BCzVBi doped CBP, ZnS, and Alq_3. Finally, LiF (0.4 nm) and MgAg (9:1 w/w) were evaporated on the top of the ETL layer. The active areas of all the OLEDs were fixed at 1 mm^2.

Figure 16(a) shows the relationship between the frequency of an applied sine wave voltage and the output relative EL intensity of the devices L and M, which consisted of ZnS and Alq_3 as ETLs, respectively. The relative EL intensity of the organic-inorganic hybrid device (device L) showed higher response speed compared to the OLED (device M). This result indicates that the low electron mobility of Alq_3 causes the low response speed. On the other word, we can realize the increased response speed utilizing the ZnS layer with high electron mobility as the ETL. This is because the response speed of the OLED is limited by the low electron mobility of organic electron transport materials, and the electron mobility of ZnS is higher than that of Alq_3

Figure 16(b) shows the influence of the sine wave voltage on the cutoff frequency for devices L and M. By comparing the devices L and M, we found that the cutoff frequency was influenced by the applied voltage for only the device L with ZnS. The low drive voltage of the OLED has been required for all the applications, such as mobile phones, flat panel displays, general lightings, and visible optical communications. This result indicates that the ZnS-ETL is important technique to improve both the response speed and the drive voltage.

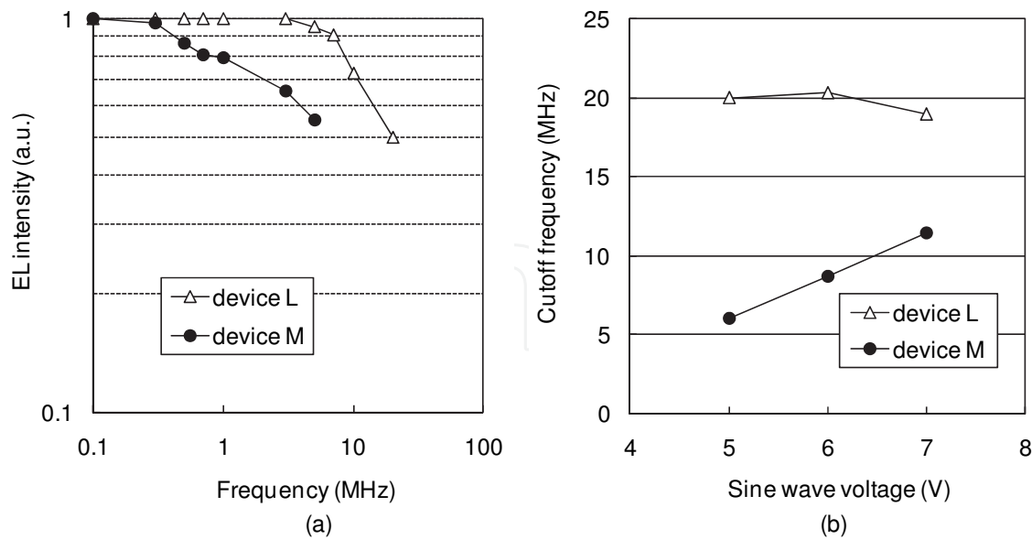

Fig. 16. (a) Relative EL intensity as a function of the applied sine wave voltage for two device with ZnS (device L) and Alq3 (device M) used as ETLs. (b) Relationship between the cutoff frequency and the sine wave voltage. (Fukuda et al., 2008a)

5. Intuitive visible data communication system with OLED as transceiver

5.1 Experimental

In this section, we show a demonstrator of the institutive visible optical communication system utilizing the OLED as an electro/optic converter. This system consisted of the transceiver module with the OLED and the pen-type receiver module with the semiconductor photo diode at a point, as shown in Fig 16. When the point of the pen-type receiver module approaches the emitting area of the OLED, you can get information from the OLED. Furthermore, the emitting area was 2 mm x 2mm, and the many people can touch without thinking the precious alignment between the pen-type receiver module and the OLED.

The fabrication process and the experimental results are discussed as bellows. We deposited cupper-phthalocyanine (CuPc) as a hole injection leayr, α-NPD as a HTL, rubrene in Alq_3 as an EML, Alq_3 as an ETL, and LiF as an EIL subsequently, upon the ITO-coated glass substrate. The device structure is glass substrate/ITO 150 nm/CuPc 10 nm/α-NPD 40 nm/1.0wt% rubrene:Alq_3 20 nm/Alq_3 40 nm/LiF 0.5 nm/Al 150 nm. Since the degradation of organic layers is caused by humidity and oxygen, the device was deposited by employing the conventional thermal evaporation at 6.0×10^{-6} Torr without breaking the vacuum. Then, the fabricated device was encapsulated under nitrogen atmosphere using UV-curable adhesives and cavity glass lids.

The inset of Fig. 16 shows the inside of the pen-type receiver module. We used driver IC (MAXIM, MAX749CSA) to apply the modulated pulse voltage. By applying the pulse voltage, the modulated optical signal generated from the emitting area of the OLED. In addition, the pen-type receiver module consisted of the photo-diode at a point, the comparator (NEC, μPC271G2), the operational amplifier (Linear Technology, LT1192 S8), and many electric parts (resistors, capacitor, and mechanical switch).

Pseudo electric signals were applied to the OLED to demonstrate the data transmission between the OLED and the photo diode. The amplitude and the clock frequency of pseudo

signals were 4 V and 1 Mbps, respectively. In addition, the bias voltage of 4 V was also applied to the OLED by a DC voltage source. Then, the pen-type receiver was approached the emitting area of the OLED, as shown in Fig. 17. Finally, the output optical signal was changed the electric signal by a photo-diode, and the time-resolved output power was measured by an oscilloscope.

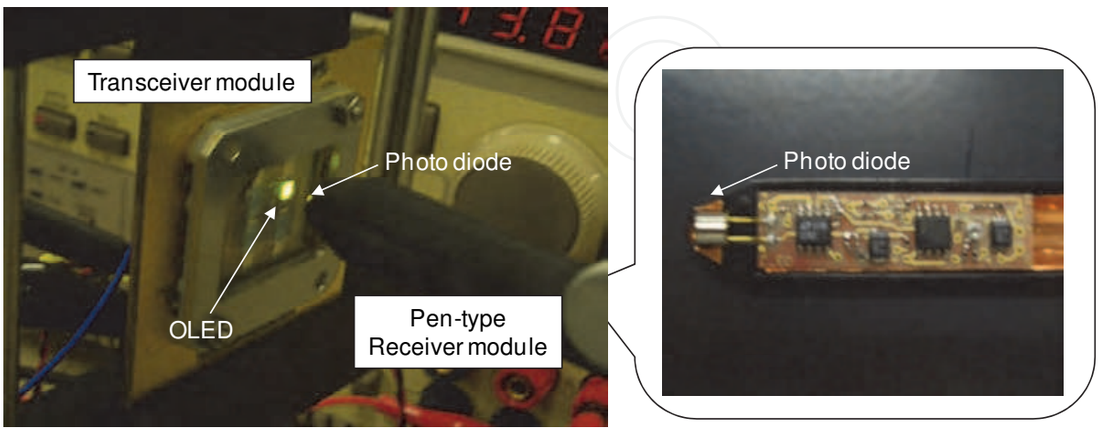

Fig. 17. (a) Demonstrator of the intuitive visible optical communication system, which consists of the OLED as a transceiver module and the pen-type receiver module. The inset shows the inside of the pen-type receiver module. (Fukuda et al., 2008b).

5.2 Result and discussions

Figure 18 shows the input electrical signal and the output optical signal as a function of the time. The output optical signal was received using the pen-type receiver module when the

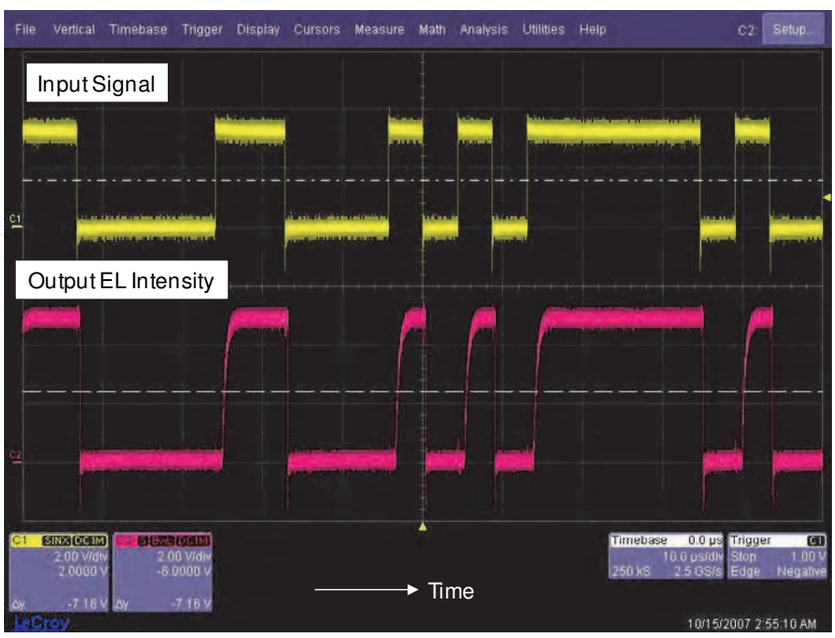

Fig. 18. Input electrical signal (yellow) and the output optical signal (pink) as a function of the time. The frequency of the input electrical signal was 1 Mbps.

pseudo-random signals were applied to the OLED. Transmission speed of pseudo-random signals was 1 Mbps. As clearly shown in Fig. 18, the rise time is larger than the decay time. This is because that the injection time of carriers from electrodes to the EML is long. However, we can realize the error-free data transmission at a speed of 1 Mbps using the transceiver module with the OLED.

6. Conclusion

In this chapter, we demonstrated fast-response OLEDs for the intuitive visible optical communications. We successfully achieved the more than 20 MHz by optimizing device parameters, such as the emitting area, the thickness of the carrier transport layer, the metal cathode, the fluorescence lifetime of the emitting material, the combination of the host-guest material, and the semiconductor ETL. Finally, we also demonstrated the demonstrator of the institutive optical data transmission system using the OLED as the transceiver. If the pen-type receiver module is touched the emitting area of the OLED, we can get the pseudo-random signals without thinking the precious alignment between the OLED and the pen-type receiver module.

7. Acknowledgment

The authors would like to thank Ms. K. Tanaka, Mr. K. Hashizume, Mr. H. Ohashi, and Mr. T. Hanawa of Nokia Research Center, Nokia Japan Co. Ltd. for their advices to practical applications of institutive visible optical communications. The authors also would like to thank Mr. H. Hosoya, Mr. Fujimaki, Mr. M. Ohashi, Mr. K. Asano, Mr. K. Azegami, Mr. Y. Terada, Mr. K. Ichii, and Mr. H. Kannno of Fujikura Ltd. for their help. The authors also would like to thank Prof. M. Ichikawa, Prof. B. Wei, Miss. T. Okada, Mr. E. Suto to do experiment and discussion. The part of this work was supported by Fujikura Ltd. And CLUSTER (the second stage) of Ministry of Ministry of Education, Culture, Sports, Science and Technology, Japan.

8. References

Adachi, C., Baldo, M.A., Thompson, M.E. & Forrest, S.R. (2001). Nearly 100% internal phosphorescence efficiency in an organic light emitting device, *J. Appl. Phys*., Vol.90: 5048-5051.

Barth, S., Müller, P., Riel, H., Seidler, P.F. & Rieb, W. (2001). Electron mobility in tris(8-hydroxyquinoline)aluminum thin films determined via transient electroluminescence from single- and multilayer organic light-emitting diodes, *J. Appl. Phys*., Vol.89: 3711-3719..

Cao. Y., Parker, I. Yu, G., Gang, Z. & Heeger, A. (1999). Improved quantum efficiency for electroluminescence in semiconducting polymers, *Nature*, Vol.397: 414-416.

Dexter, D. (1953). A theory of sensitized luminescence in solids, *J. Chem. Phys*., Vol.21: 836-850.

Eisenthal, K.B., Siegel, S. (1964). Influence of Resonance Transfer on Luminescence Decay, *J. Chem. Phys*., Vol.41: 652-655.

Fukuda, T., Ohashi M., Wei, B., Okada, T., Ichikawa, M. & Taniguchi, Y. (2007). Transient response of blue organic electroluminescence devices with short fluorescence

lifetime of substituted phenyl/vinyl compound as an emissive layer, *Opt. Lett.*, Vol.32: 1150-1152.

Fukuda, T., Okada, T., Wei, B., Ichikawa, M. & Taniguchi, Y. (2007). Transient property of optically pumped organic film of different fluorescence lifetimes, *Appl. Phys. Lett.*, Vol.90: 231105.

Fukuda, T., Okada, T., Wei, B., Ichikawa, M. & Taniguchi, Y. (2007). Influence of carrier-injection efficiency on modulation rate of organic light source, *Opt. Lett.*, Vol.32: 1905-1907.

Fukuda, T., Wei, B., Ichikawa, M. & Taniguchi, Y. (2007). Enhanced Modulation Speed of Tris(8-hydroxyquinoline)aluminium-Based Organic Light Source with Low-Work-Function Electrode, *Jpn. J. Appl. Phys.*, Vol.46: 7880-7884.

Fukuda, T., Wei, B., Ichikawa, M. & Taniguchi, Y. (2007). Effect of Hole and Electron Injection Time on Modulation Speed of Organic Light-Emitting Diode, *Abstract of the 13th microoptics conference 2007*, pp.154-155, Kagawa, Japan, Oct. 2007.

Fukuda, T., Okada, T., Wei, B., Ichikawa, M. & Taniguchi, Y. (2008). Fast-response hybrid organic-inorganic light-emitting diode, *Phys. Status Sol.: Rap. Res. Lett.*, Vol.2: 290-292.

Fukuda, T. & Taniguchi, Y. (2008). Fast response organic light-emitting diode for visible optical communication, *Proceedings of SPIE*, Vol.6899: 68990K-1-83990K-13.

Fukuda, T., Wei, B., Ichikawa, M. & Taniguchi, Y. (2009). Transient characteristics of organic light-emitting diode with efficient energy transfer in emitting material, *Thin Solid Films*, Vol.518: 567-570.

Hatton, R.A., Day, S.R., Chesters, M.A. & Willis, M.R. (2001). Organic electroluminescent devices: enhanced carrier injection using an organosilane self assembled monolayer (SAM) derivatized ITO electrode, *Thin Solid Films*, Vol.394: 292-297.

Hung, L.S., Tang, C.W. & Mason, M.G. (1997). Enhanced electron injection in organic electroluminescence devices using an Al/LiF electrode, *Appl. Phys. Lett.*, Vol70: 152-154.

Ichikawa, M., Amagai, J., Horiba, Y., Koyama, T. & Taniguchi, Y. (2003). Dynamic turn-on behavior of organic light-emitting devices with different work function cathode metals under fast pulse excitation, *J. Appl. Phys.*, Vol.94: 7796-7800.

Ichikawa, M., Kawaguchi, T., Kobayashi, K., Miki, T., Furukawa, K., Koyama, T. & Taniguchi, Y. (2006). Bipyridyl oxadiazoles as efficient and durable electron-transporting and hole-blocking molecular materials, *J. Mater. Chem.*, Vol.16: 221-225.

Kajii, H., Tsukagawa, T., Taneda, T. & Ohmori, Y. (2002). Application of Organic Light Emitting Diode Based on the Alq_3 Emissive layer to the Electro-Optical Conversion Device, *IEICE Trans. Electron.*, vol.E85-C: 1245-1246.

Kajii, H., Tsukagawa, T., Taneda, T., Yoshino, K., Ozaki, M., Fujii, A., Hikita. M., Tomaru, S., Imamura, S., Takenaka, H., Kobayashi, J., Yamamoto, F. & Ohmori, Y. (2002). Transient Properties of Organic Electroluminescent Diode Using 8-Hydroxyquinoline Aluminum Doped with Rubrene as an Electro-Optical Conversion device for Polymeric Integrated devices, *Jpn. J. Appl. Phys.*, Vol.41: 2746-2747.

Kampen, T., Bekkali, A., Thurzo, I., Zahn, D.R.T., Bolognesi, A., Ziller, T., Carlo, A.D. & Lugli, P., (2004). Barrier height of organic modified Schottky contacts:theory and experiment, *Appl. Surf. Sci.*, Vol.234: 313-320.

Kido, J. & Matsumoto, T. (1998). Bright organic electroluminescent devices having a metal-doped electron-injecting layer, *Appl. Phys. Lett.*, Vol.73: 2866-2868.

Kim, J.-S. Kajii, H. & Ohmori, Y. (2006). Characteristics of optical response in red organic light-emitting diodes using two dopant systems for application to the optical link devices, *Thin Solid Films*, Vol.499: 343-348.

Kin, Z., Yoshihara, K., Kajii, H., Hayashi, K. & Ohmori, Y. (2006). Effects of CsF/Metal Interface on Electron Injection in Polymer Light-Emitting Diodes, *Jpn. J. Appl. Phys.*, Vol.45: 3737-3741.

Koike, Y. (2008). Microoptics and Photonics Polymer, Jpn. J. Appl. Phys., Vol.47: 6629-6634.

Mignonneau, L. & Sommerer, C. (2005). Designing emotional, metaphoric, natural and intuitive interfaces for interactive art, edutainment and mobile communications, *Computers & Graphics*, Vol.29: 837-851.

Mori, K., Ning, T., Ichikawa, M., Koyama, T. & Taniguchi, Y. (2003). Organic Light-Emitting Devices Patterned by Screen Printing, *Jpn. J. Appl. Phys.*, Vol.39: L942-L944.

Morimune, T., Kajii, H. & Ohmori, Y. (2006). High-Speed Organic Photodetectors Using Heterostructure with Phthalocyanine and Perylene Derivative, *Jpn. J. Appl. Phys.*, Vol.45: 546-549.

Morrison, G.D. (2005). A Camera-Based Input Device for Large Interactive Displays, *IEEE Comput. Grap. Appl.* Vol.23: 52-57.

Nüesch, F., Kamaraś, K. & Zuppiroli, L. (1998). Protoned metal-oxide electrode for organic light emitting diodes, *Chem. Phys. Lett.*, Vol.283: 194-200.

Ooe, M., Satoh, R., Naka, S., Okada, H. & Onnagawa, H. (2003). Painting Method for Organic Electroluminescent Devices, *Jpn. J. Appl. Phys.*, Vol.42: 4529-4534.

Panchaphongsaphak, B., Burgkart, R. & Riener, R. (2007). Three-Dimensional Touch Interface for Medical Education, *IEEE Trans. Info. Tech. BioMed.* Vol.11: 251-263.

Parker, I.D. (1994). Carrier tunnelling and device characteristics in polymer light-emitting diodes, *J. Appl. Phys.*, Vol.75: 1656-1666.

Shimada, H., Yanagi, J., Matsushita, Y., Naka, S., Okada, H. & Onnagawa, H. (2006). Organic Multifunction Diodes Operable for Emission and Photodetection Modes, *Jpn. J. Appl. Phys.*, Vol.45: 3750-3753.

Stöβel, M., Staudigel, J., Steuber, F., Blässing, J. Simmerer, J. Winnacker, A., Neuner, H., Metzdorf, D., Johannes, H.-J. & Kowalsky, W. (2000). Electron injection and transport in 8-hydroxyquinoline aluminium, *Synth. Met.*, Vol.111-112: 19-24.

Tang, C.W. & VanSlyke, S.A. (1987). Organic electroluminescent diodes, *Appl. Phys. Lett.*, Vol.51: 913-915.

Tsutsui, T. (1997). Recent progress of molecular organic electroluminescent materials and devices, *MRS Bulletin*, Vol.22: 39-45.

Uchida, M., Izumisawa, T., Nakano, T., Yamaguchi, S., Tamao, K. & Furukawa, K. (2001). Structural Optimization of 2,5-Diarylsiloles as Excellent Electron-Transporting Materials for Organic Electroluminescent Devices, *Chem. Mater.*, Vol.13: 2680-2683.

Wei, B., Furukawa, K., Amagai, J., Ichikawa, M., Koyama, T. & Taniguchi, Y. (2004). A dynamic model for injection and transport of charge carriers in pulsed organic light-emitting diodes, *Semicond. Sci. Technol.*, Vol.19: L56-L59.

Xu, Q., Ouyang, J., Yang, Y. Ito, T. & Kido, J. (2003). Ultrahigh efficiency green polymer light-emitting diodes by nanoscale interface modification, *Appl. Phys. Lett.*, Vol.83: 4695-4697.

Zheng, X., Wu, Y., Sun, R., Zhu, W., Jiang, X., Zhang, Z. & Xu, S. (2005). Efficiency improvement of organic light-emitting diodes using 8-hydroxy-quinolinato lithium as an electron injection layer, *Thin Solid Films*, Vol.478: 252-255.

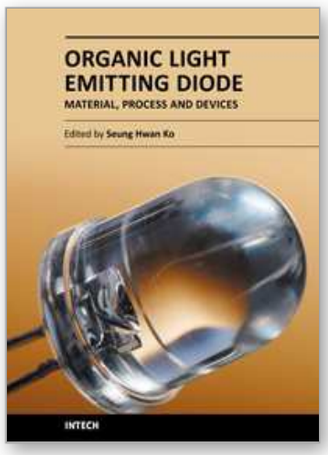

Organic Light Emitting Diode - Material, Process and Devices

Edited by Prof. Seung Hwan Ko

ISBN 978-953-307-273-9
Hard cover, 322 pages
Publisher InTech
Published online 27, July, 2011
Published in print edition July, 2011

This book contains a collection of latest research developments on Organic light emitting diodes (OLED). It is a promising new research area that has received a lot of attention in recent years. Here you will find interesting reports on cutting-edge science and technology related to materials, fabrication processes, and real device applications of OLEDs. I hope that the book will lead to systematization of OLED study, creation of new research field and further promotion of OLED technology for the bright future of our society.

How to reference

In order to correctly reference this scholarly work, feel free to copy and paste the following:

Takeshi Fukuda and Yoshio Taniguchi (2011). Fast-Response Organic Light-Emitting Diode for Interactive Optical Communication, Organic Light Emitting Diode - Material, Process and Devices, Prof. Seung Hwan Ko (Ed.), ISBN: 978-953-307-273-9, InTech, Available from: http://www.intechopen.com/books/organic-light-emitting-diode-material-process-and-devices/fast-response-organic-light-emitting-diode-for-interactive-optical-communication

INTECH
open science | open minds

InTech Europe
University Campus STeP Ri
Slavka Krautzeka 83/A
51000 Rijeka, Croatia
Phone: +385 (51) 770 447
Fax: +385 (51) 686 166
www.intechopen.com

InTech China
Unit 405, Office Block, Hotel Equatorial Shanghai
No.65, Yan An Road (West), Shanghai, 200040, China
中国上海市延安西路65号上海国际贵都大饭店办公楼405单元
Phone: +86-21-62489820
Fax: +86-21-62489821

IntechOpen